

Published in final edited form as:

Metabolism. 2013 June ; 62(6): 873–887. doi:10.1016/j.metabol.2013.01.001.

Expression of p27Kip1, a cell cycle repressor protein, is inversely associated with potential carcinogenic risk in the genetic rodent models of obesity and long-lived Ames dwarf mice

Isao Eto*

Department of Nutrition Sciences, University of Alabama at Birmingham, 316 Susan Mott Webb Nutrition Sciences Building, 1675 University Boulevard, Birmingham, AL 35294, USA

Abstract

Introduction—The association of genetic rodent models of obesity and cancer still remains a controversial issue. Although this controversy has largely been resolved in recent years for homozygous leptin receptor-deficient obese Zucker rats and homozygous long-lived Ames dwarf mice, it is still unresolved for homozygous leptin-deficient obese ob/ob mice.

Objective—The objective of the present study described below was to investigate whether the expression of the cell cycle repressor protein p27(Kip1) is (a) down-regulated in the tumor-free homozygous leptin receptor-deficient obese Zucker rats as well as tumor-free homozygous leptin-deficient obese ob/ob mice and (b) up-regulated in the tumor-free homozygous long-lived Ames dwarf mice.

Methods—To achieve this objective, we first performed western immunoblot analysis of the hepatic expression of p27. We then performed western immunoblot analysis and proteomic analysis of the hepatic expression of the proteins involved in the upstream molecular signaling pathways for the expression of p27. Lastly, we analyzed the serum levels of glucose, insulin, and branched-chain amino acids, all of which have been shown to regulate, causally and inversely, the expression of p27.

Results/Conclusions—The results indicated that the hepatic expression of p27 was down-regulated in the homozygous leptin receptor-deficient obese Zucker rats and up-regulated in the homozygous long-lived Ames dwarf mice as expected. We also found that the hepatic expression of p27 was down-regulated in the homozygous leptin-deficient obese ob/ob mice. This last observation was not completely consistent with all of the results of the published studies where homozygous leptin-deficient obese ob/ob mice were used.

Keywords

Cancer; Glucose; Insulin; Branched-chain amino acids

© 2013 Elsevier Inc. All rights reserved.

*Tel.: +1 205 934 4099; fax: +1 205 934 7049. etoi@uab.edu.

Ethical statement

Prior to the commencement of this study, all procedures involving rodents were reviewed and approved by the Institutional Animal Care and Use Committee (IACUC) at the University of Alabama at Birmingham (Birmingham, AL, USA).

Conflicts of interest

We declare that no actual or potential conflicts of interest exist that might, in principle, influence our scientific judgment.

1. Introduction

The association of genetic rodent models of obesity and cancer is a complicated and sometimes controversial issue. One of the non-controversial genetic rodent models of obesity is the homozygous leptin receptor-deficient obese Zucker rats. It was reported in 2005 that female obese Zucker rats exhibited increased incidence of 7,12-dimethylbenz(a)anthracene (DMBA)-induced rat mammary adenocarcinomas compared with female lean control Zucker rats [1–7].

By contrast, it has been a controversial issue for homozygous leptin-deficient obese ob/ob mice. On the one hand, it was reported that the RM1 murine prostate cancer cells, injected subcutaneously into the obese ob/ob mice, were significantly larger compared with lean control mice [8]. On the other hand, it was also reported that the growth of the MMTV-Wnt-1 mammary tumors, orthotopically transplanted into the right mammary fat pad of obese ob/ob mice, were suppressed compared with lean control mice [9]. Thus, diametrically opposed observations were reported with these mice.

The homozygous long-lived Ames dwarf mice have physiological characteristics that are similar to the effects of dietary restriction [10]. Ames dwarf mice were reported in 2003 to have a delayed occurrence of presumably fatal neoplastic disease compared with their normal siblings [10]. In addition, the incidence of presumably fatal adenocarcinomas in lung was reported to be significantly lower in Ames dwarf mice than for their normal siblings [10,11]. These observations on the Ames dwarf mice were based on the decreased occurrence of the spontaneous tumors [10,11]. We are not aware of a report on the responses of the Ames dwarf mice to the chemical carcinogens, but the Snell dwarf mice (which are phenotypically very similar to Ames dwarf mice) were reported to be resistant to chemical carcinogens [12], suggesting that in the dwarf mice the risk of developing cancer is generally decreased regardless of whether the tumors occur spontaneously or are induced by chemical carcinogens.

The study described below resulted from our attempts to re-examine the controversies surrounding the association of genetic rodent models of obesity and cancer from a fresh perspective of the regulation of the expression of p27 (Kip1) in the tumor-free host rodents. More specifically, the objective of our study was to investigate whether the expression of p27 is (a) down-regulated in the tumor-free homozygous leptin receptor-deficient obese Zucker rats as well as tumor-free homozygous leptin-deficient obese ob/ob mice and (b) up-regulated in the tumor-free homozygous long-lived Ames dwarf mice.

p27 is a cell cycle repressor protein that is expressed variably but ubiquitously in various tissues from rats and mice. It is a member of the family of cyclin-dependent kinase (CDK) inhibitors (CDIs) [13]. When down-regulated, p27 up-regulates the activities of certain cyclin/CDK complexes, thereby increasing the cell cycle progression from G1 to S phase, DNA replication, and the risk of developing cancer. Conversely, when up-regulated, p27 down-regulates the activities of certain cyclin/CDK complexes, thereby decreasing the cell cycle progression from G1 to S phase, DNA replication, and the risk of developing cancer. Thus, p27 could act as either a pro or anti-cancer promotion protein, provided that the target cells have either already been initiated or are being initiated by carcinogens.

With regard to the risk of developing cancer, p27 exhibits a set of unique characteristics that are not seen in any other G1-to-S phase cell cycle regulatory proteins [14–16]. First, a relatively large number of nutritional and chemopreventive anti-cancer agents specifically increase the expression of p27 without directly affecting the expression of any other G1-to-S phase cell cycle regulatory proteins including INK4s, p57(Kip2), p21(Cip1Waf1), D-type cyclins, cyclin E, cyclin A, CDK2, CDK4 and CDK6 [14]. Second, the degree of increase in

the expression of p27 in human breast adenocarcinoma cells *in vitro* is linearly and positively associated with the degree of inhibition of methylnitrosourea (MNU)-induced rat mammary adenocarcinoma *in vivo* [15]. This association, of course, does not exist for some anti-cancer agents that could not be converted to active anti-cancer metabolites *in vitro*. Lastly, unlike any other G1-to-S phase cell cycle regulatory proteins, expression of p27 is regulated primarily at the level of translation, not at the level of transcription [14–20]. For example, the level of expression of p27 “protein” oscillates significantly during the cell cycle, but the expression of p27 “mRNA” does not. It was proposed that the expression of p27 could also be regulated by various post-translational mechanisms, including ubiquitin-proteasome-induced degradation [21–24], complex association [25], subcellular localization [26–31], and protein phosphorylation [31–33].

As described below, our new approach has enabled us to largely resolve the controversies surrounding the association of genetic rodent models of obesity and cancer with only a few exceptions. We believe that this study has a strong translational potential.

2. Materials and methods

2.1. Animals

All procedures involving animals were reviewed and approved by the Institutional Animal Care and Use Committee (IACUC) at the University of Alabama at Birmingham (Birmingham, AL, USA). All animals were housed in regular rat/mouse cages on 12-h light/dark cycle (lights on at 7:00 am) and had unlimited access to food and tap water at our institution. They were all sacrificed – tumor-free – at 12 weeks of age after overnight fast and the serum and liver samples were collected from each animal, snap-frozen in liquid nitrogen, and stored at –80 °C until processed further.

Homozygous leptin-receptor deficient obese Zucker (*Lep^r fa/fa*) rats (males) and heterozygous lean control Zucker (*Lep^r Fa/fa*) rats (males) were purchased from the Charles Rivers Associates (Boston, MA, USA) at 9 to 10 weeks of age.

Homozygous leptin-deficient obese ob/ob mice (males) and heterozygous lean control mice (males) were purchased from the Jackson Laboratory (Bar Harbor, MI, USA) at 9 to 10 weeks of age.

Homozygous long-lived Ames dwarf (*Prop¹ ^{-/-}*) mice (males) and heterozygous Ames normal control (*Prop¹ ^{+/-}*) mice (males) were purchased initially from the Jackson Laboratory (Bar Harbor, MI, USA) at 9 to 10 weeks of age, but later they were kindly and generously provided by Dr. Andrzej Bartke at the Southern Illinois University (SIU) School of Medicine (Springfield, IL, USA).

Homozygous Apoe^{tm1Unc} mutant mice on C57BL/6J background (males) and wild-type C57BL/6J mice (males) were purchased from the Jackson Laboratory (Bar Harbor, MI, USA) at 9 to 10 weeks of age.

At our institution, Zucker rats were fed Purina Rodent Chow Diet 5002, which contained approximately 23% protein and included ground corn, dehulled soybean meal, fish meal, and porcine meat meal. On the other hand, all mice were fed Lab Diet ®5K52, which contained approximately 19% protein and included ground wheat, dehulled soybean meal, and fish meal.

2.2. Western immunoblot analysis

The following primary antibodies were purchased from the Cell Signaling Technology (Danvers, MA, USA): (a) 4E-BP1 (total) and phospho-4E-BP1 (Ser65 and Thr37/46); (b) S6K1 (total) and phospho-S6K1 (Thr389), (c) SIRT3, (d) p27Kip1, (e) AMPK α (total) and phospho-AMPK α , (Thr172) and (f) GAPDH. Additionally, the following primary antibodies were obtained from the Santa Cruz Biotechnology (Santa Cruz, CA, USA): (a) GAPDH and (b) p27Kip1.

Western immunoblot analysis of the expression of p27(Kip1) and the upstream molecular signaling pathways for the expression of p27 was performed using rodent livers. The soluble protein extracts from the rodent livers were sonicated in RIPA Lysis Buffer (Santa Cruz Biotechnology, Santa Cruz, CA, USA) containing PMSF, sodium orthovanadate and protease inhibitor cocktail and supplemented with 50 mmol/L NaF. The soluble protein extracts were collected by centrifugation and stored at -80°C until processed for western immunoblot analysis.

For western immunoblot analysis, the soluble protein extracts (35 to 50 μg protein per lane) were applied to the SDS-PAGE and, after fractionation, proteins were transferred to the nitrocellulose membrane, which was then blocked and incubated in a solution containing first primary antibody. After shaking overnight at 4°C , the target proteins bound to the first primary antibody were further incubated in a solution containing alkaline phosphatase (AP)-conjugated secondary anti-immunoglobulin antibody and detected by chemiluminescence using TROPIX Western-Star Kit (Applied Biosystems, Foster City, CA, USA). After exposure to X-ray film, the blots were stripped using Western Re-Probe Solution (G-Biosciences, St. Louis, MO, USA), checked for removal of the chemiluminescence and then re-probed with second primary antibody.

Densitometric measurements of the intensity of the bands on the X-ray films were performed using UN-SCAN-IT Gel & Graph Digitizing Software Version 6.1 (Silk Scientific, Orem, UT, USA). Background corrections were done by four corner interpolation method and optical density calculations were performed using linear standard reflective scan method.

2.3. Proteomic analysis

The overall workflow of the proteomic analysis of the liver samples is shown in Fig. 1. The cryosectioned samples were subjected to (a) hematoxylin and eosin (H & E) staining and (b) differential proteomic profiling analysis by direct matrix-assisted laser desorption/ionization (MALDI) time-of-flight (TOF) mass spectrometry (MS). The homogenized – rather than the cryosectioned – liver samples were subjected to the differential proteomic identification analysis by nano liquid chromatography–tandem mass spectrometry (nano LC-MS/MS). Nano LC-MS/MS method was used because it tended to produce far smaller number of false positives than the conventional two dimensional (2D)-Gel method. These analyses were performed by Drs. James A. Mobley and Senait G. Asmellash at the Urologic and Clinical Proteomics Research Facility at the University of Alabama at Birmingham (Birmingham, Alabama, U.S.A.).

Searches for the differential identifications of the nano LC-MS/MS-generated protein data were all carried out as follows using species-specific subsets of the UniRef database: All tandem mass spectrometry data were converted to mzXML format using instrument-specific converting software packages 48 (Institute for Systems Biology, Seattle, Washington & Fred Hutchinson Cancer Center) and run through SEQUEST, X!TANDEM, and MASCOT separately. X!TANDEM was downloaded from The Global Proteome Machine Organization, while licenses were purchased for the other two search engines (ThermoFisher

for SEQUEST, and Matrix Science, Boston, MA, for MASCOT). All three of these top matching algorithms were utilized in order to increase confidence in protein identifications, while also decreasing the propensity for false negatives. These data were then “combined” and analyzed using protein Prophet (also from ISB, above), which was capable of utilizing all of these data from each output to determine a “best fit” for a specific peptide fragmentation pattern as it related to an appropriate match from a large database with high confidence. Cut off filters for protein Prophet varied depending on a dynamically generated probability score that was determined based on each data set. In addition, this approach calculated a true positive correlation as opposed to simply a false positive, common to other approaches. This was important since sample characteristics could change from run to run and since Prophet took into account both true and false-positives and therefore a more accurate probability score can be determined.

Final analysis was then carried out using Expressionist software from Genedata. This package allowed the aligning of mass and time tags from ion plots generated from the post LC/MS run. Much like 2D PAGE software packages, a background subtraction, normalization, and peak detection could be carried out. This was then followed by common statistical analysis to search for disease relevant proteins correlating with a clinical endpoint. The protein ID's generated from the DB searches were tied to this analysis and carried on to the final list of potential proteins of interest.

2.4. Analysis of the serum levels of glucose, insulin, triglycerides and free amino acids

Serum levels of glucose, insulin, and triglycerides were determined at our laboratory (Department of Nutrition Sciences, University of Alabama at Birmingham (UAB)) (Birmingham, AL, USA). This laboratory has been jointly operated by the NIH-funded Pittman General Clinical Research Center and Nutrition Obesity Research Center at UAB.

Glucose was determined by glucose oxidase method. Insulin was determined by double-antibody radioimmunoassay procedure using RIA Linco kits manufactured by the Linco Research (St. Charles, MO, USA). Triglycerides were determined by glycerylphosphate oxidase (GPO) method using Stanbio Triglyceride LiquiColor kits manufactured by Stanbio Laboratory (Boerne, TX, USA).

Serum levels of free amino acids were determined at the University of California Davis Molecular Structure Facility (Davis, CA, USA) using Model L-8900 Amino Acid Analyzer (Hitachi High Technologies America, San Jose, CA, USA), Li-Ion Exchange Column (Pickering Laboratories, Mountain View, CA, USA) and EZChrome Elite software (Hitachi High Technologies America, San Jose, CA, USA).

2.5. Statistical analysis

An experimental value with statistical significance of $P < 0.05$ compared to the control by t test is indicated as either a single asterisk or actual P value on top of the vertical bar.

3. Results

To assess the regulation of the expression of p27, we used the following three groups of rodents (tumor-free males sacrificed at 12 weeks of age), namely (a) homozygous leptin receptor-deficient obese Zucker rats and heterozygous lean control Zucker rats, (b) homozygous leptin-deficient obese ob/ob mice and heterozygous lean control mice, and (c) homozygous long-lived Ames dwarf mice and heterozygous Ames normal control mice. These animals were “tumor-free” based on the following two criteria: (1) they were generally tumor free at this young age as confirmed by our resident pathologist and the commercial suppliers and also (2) they were not treated with chemical carcinogens.

Additionally, only male rats and mice were used in this study because the differences of sex did not appear to exert any significant effects on p27 expression.

3.1. Levels of the hepatic expression of p27

Homozygous leptin receptor-deficient obese Zucker rats and homozygous leptin-deficient obese ob/ob mice had significantly higher body weights (Fig. 2A and C) and the levels of the hepatic expression of p27 were significantly lower (Fig. 2B and D) in these obese rats and mice compared with heterozygous lean control rodents. These results suggested that, since p27 is expressed variably but ubiquitously in various tissues from rats and mice, the lower levels of the expression of p27 in these obese rodents could generally be responsible for increasing the risk of developing cancer (Fig. 2E).

By contrast, the homozygous long-lived Ames dwarf mice had significantly lower body weights (Fig. 3A) and the levels of the hepatic expression of p27 were significantly higher (Fig. 3B) in these dwarf mice compared with Ames normal control mice. These results suggested that the higher levels of the expression of p27 in these dwarf mice might generally be responsible for decreasing the risk of developing cancer (Fig. 3C).

3.2. Western immunoblot analysis of the hepatic activities of the upstream molecular signaling pathways for the expression of p27

Outline of the upstream molecular signaling pathways for the expression of p27 is shown in Fig. 4E for your reference [14–16].

Hepatic expression of the eukaryotic translation initiation factor 4E (eIF4E) binding protein 1 (4E-BP1) phosphorylated at Ser65 was significantly increased, relative to the total 4E-BP1, in the homozygous leptin receptor-deficient obese Zucker rats compared with lean control Zucker rats (Fig. 4A and B). Furthermore, hepatic expression of the Akt/protein kinase B (PKB) phosphorylated at Thr308 was also significantly increased, relative to the total Akt/PKB, in the homozygous leptin receptor-deficient obese Zucker rats compared with lean control Zucker rats (Fig. 4C and D).

Likewise, hepatic expression of the 4E-BP1 phosphorylated at Thr37/46 was significantly increased, relative to the total 4E-BP1, in the homozygous leptin-deficient obese ob/ob mice compared with heterozygous lean control mice (Fig. 5A and B). Additionally, hepatic expression of the S6 kinase 1 (S6K1) phosphorylated at Thr389 was also significantly increased, relative to the total S6K1, and the hepatic expression of the 5'-AMP activated protein kinase alpha (AMPK α) phosphorylated at Thr172 was significantly decreased, relative to the total AMPK α , in these obese ob/ob mice compared with heterozygous lean control mice (Fig. 5C to F).

By contrast, directions of the hepatic expression of these proteins were opposite in the homozygous long-lived Ames dwarf mice compared with obese rats and mice (Fig. 5A to F), indicating that the upstream molecular signaling pathways for the expression of p27 were up-regulated in these dwarf mice compared with normal control mice.

In summary, the activities of the upstream molecular signaling pathways for the expression of p27 were (a) downregulated in the homozygous leptin receptor-deficient obese Zucker rats and homozygous leptin-deficient obese ob/ob mice and (b) up-regulated in the homozygous long-lived Ames dwarf mice.

Incidentally, hepatic expression of the mitochondrial anti-aging, anti-metabolic SIRT3 was significantly increased in the homozygous long-lived Ames dwarf mice compared with heterozygous Ames normal control mice (Fig. 5G). This observation was consistent with a

reported increase in the average life span of approximately 50% to 60% in the long-lived Ames dwarf mice compared with their normal siblings [10,11]. By contrast, hepatic expression of SIRT3 was unexpectedly unchanged in the homozygous leptin-deficient obese ob/ob mice compared with heterozygous lean control mice (Fig. 5G).

3.3. Proteomic analysis of the hepatic activities of the upstream molecular signaling pathways for the expression of p27

The hepatic activities of the upstream molecular signaling pathways for the expression of p27 were investigated further by proteomic analysis. The results of the differential proteomic identification analysis by nano liquid chromatography–tandem mass spectrometry (nano LC-MS/MS) indicated that hepatic expression of ATP synthase (Complex V in the mitochondrial oxidative phosphorylation chain) was (a) most significantly down-regulated in the homozygous leptin-deficient ob/ob mice compared with the heterozygous lean control mice (Fig. 6C) and, conversely, (b) most significantly up-regulated in the homozygous long-lived Ames dwarf mice compared with the heterozygous Ames normal control mice (Fig. 6E). These results were consistent with the direction of the changes in the 5'-AMP-activated protein kinase alpha (AMPK α) phosphorylated at Thr172 described above. Additionally, nano LC-MS/MS analysis revealed that the fructose-bisphosphate aldolase and apolipoprotein C-III were down-regulated in the livers of homozygous long-lived Ames dwarf mice compared with normal control mice (Fig. 6F). Based on the findings reported in 2001, hepatic expression of these two proteins could be down-regulated due to the up-regulation of the phosphorylated AMPK and consequent down-regulation of the hepatocyte nuclear factor 4 α (HNF-4 α) [34,35]. Thus, both of these results obtained by nano LC-MS/MS analysis suggested that the phosphorylation of AMPK was down-regulated in the homozygous leptin-deficient obese ob/ob mice and, conversely, up-regulated in the homozygous long-lived Ames dwarf mice.

In summary, the results of the nano LC-MS/MS analysis also indicated that the activities of the upstream molecular signaling pathways for the expression of p27 were (a) down-regulated in the homozygous leptin-deficient ob/ob mice compared with heterozygous lean control mice and (b) up-regulated in the homozygous long-lived Ames dwarf mice compared with heterozygous Ames normal control mice (see Fig. 4E for your reference).

Hematoxylin and eosin (H & E) staining of the livers of the homozygous leptin-deficient ob/ob mice indicated that they were loaded with many fat droplets (Fig. 6A). Fatty livers were also observed in the homozygous leptin receptor-deficient obese Zucker rats (H & E staining images not shown).

3.4. Analysis of the serum levels of glucose, insulin, triglycerides and free amino acids

Extracellular concentrations of (a) glucose, (b) insulin, or (c) branched-chain amino acids have previously been shown to regulate, causally and inversely, the expression of p27 (see Fig. 4E for your reference) [14–16].

Serum concentrations of glucose and insulin were significantly increased in the homozygous leptin receptor-deficient obese Zucker rats compared with heterozygous lean control Zucker rats (Fig. 7A and B). Likewise, the serum concentrations of glucose, insulin, and certain branched-chain amino acids (i.e., valine and isoleucine) were significantly increased in the homozygous leptin-deficient obese ob/ob mice compared with heterozygous lean control mice (Fig. 7D and E and Table 1). By contrast, the serum concentrations of glucose, insulin, valine and isoleucine were significantly decreased in the homozygous long-lived Ames dwarf mice compared with heterozygous Ames normal control mice (Fig. 7D and E and Table 1).

These results indicated again that the expression of p27 was (a) down-regulated in the homozygous leptin receptor-deficient obese Zucker rats and homozygous leptin-deficient obese ob/ob mice and (b) up-regulated in the homozygous long-lived Ames dwarf mice.

The serum levels of alanine were also significantly increased in the homozygous leptin-deficient obese ob/ob mice compared with heterozygous lean control mice (Table 1) and significantly decreased in the homozygous long-lived Ames dwarf mice compared with heterozygous Ames normal control mice (Table 1). These changes in the serum levels of alanine might be correlated with the changes in the serum levels of lactate – and potentially the levels of pyruvate – in these mice (data not shown).

Although the serum levels of leucine, phenylalanine and some other amino acids were significantly increased in the homozygous leptin-deficient obese ob/ob mice, they were not significantly decreased in the homozygous long-lived Ames dwarf mice (Table 1).

The question of whether increased serum concentrations of triglycerides (Fig. 7C) could down-regulate the expression of p27 was investigated next.

3.5. Serum levels of triglycerides and the hepatic expressions of p27 and 4E-BP1 phosphorylated at Ser65 in homozygous *ApoE*^{tm1Unc} mutant mice

Apolipoprotein E (ApoE) has an important role in triglyceride metabolism and an increase in the serum triglyceride levels was reported in the mice homozygous for the *ApoE*^{tm1Unc} mutation on C57BL/6 background. These considerations led us to use these mice to investigate whether increased concentrations of serum triglycerides could be associated with down-regulation of the expression of p27. The results indicated that, even though the serum concentrations of triglycerides were significantly increased in these mutant mice compared with wild-type control mice (Fig. 8A), the hepatic expression of p27 was unchanged (Fig. 8B) and the expression of the 4E-BP1 phosphorylated at Ser65 was also unchanged, relative to the total 4E-BP1 (Fig. 8C and D), in the homozygous *ApoE*^{tm1Unc} mutant mice compared with wild-type C57BL/6 control mice. These results suggested, at least, that the increased concentrations of serum triglycerides might not be associated with down-regulation of the expression of p27.

We did not measure the serum levels of triglycerides in either ob/ob or Ames dwarf mice. However, like obese Zucker rats, dyslipidemia secondary to obesity was also reported in ob/ob mice [37]. In Ames dwarf mice, the serum levels of triglycerides were significantly decreased, but the levels of triglycerides in the liver and skeletal muscle were significantly elevated [38].

4. Discussion

The observations presented above indicated that the expression of p27 was (a) down-regulated in the homozygous leptin receptor-deficient obese Zucker rats and homozygous leptin-deficient obese ob/ob mice compared with their respective lean controls and (b) up-regulated in the homozygous long-lived Ames dwarf mice compared with normal control mice. It is likely that these changes in the expression of p27 were achieved by the changes in the regulation of the upstream molecular signaling pathways for the expression of p27 and by the changes in the serum concentrations of glucose, insulin, valine or isoleucine.

These changes in the regulation of the expression of p27 were consistent with the increased risk of developing cancer in homozygous leptin receptor-deficient obese Zucker rats [1–7] and the decreased risk of developing cancer in homozygous long-lived Ames dwarf mice as expected [10,11]. These changes were, however, not entirely consistent with the reported

risk of developing cancer in homozygous leptin-deficient obese ob/ob mice [8,9]. On the one hand, our observations were generally consistent with the results of the previously reported study where RM1 murine prostate cancer cells were injected subcutaneously into the obese ob/ob mice [8]. This study found positive associations among obesity, cancer and the serum levels of insulin. On the other hand, our observations were not entirely consistent with the results of another study where MMTV-Wnt-1 mammary tumors were orthotopically transplanted into the right mammary fat pad of obese ob/ob mice [9]. This study found negative associations between obesity and cancer, although it did find positive associations between obesity and the serum levels of insulin.

The controversial associations between genetic rodent models of obesity and cancer were not limited to the obese ob/ob mice. They were also controversial with homozygous leptin receptor-deficient obese db/db mice. On the one hand, it was reported that negative associations were found between obesity and cancer in the study where RM1 murine prostate cancer cells were injected subcutaneously into the obese db/db mice [8]. This study found that the serum levels of insulin in both obese db/db mice and lean control mice were low and not statistically different from each other [8]. On the other hand, it was also reported that neither positive nor negative associations were found between obesity and cancer in the study where MMTV-Wnt-1 mammary tumors were orthotopically transplanted into the right mammary fat pad of obese db/db mice, although the serum levels of insulin were significantly higher in obese db/db mice compared with the lean control mice [9].

While our study had been in progress, insulin had been reported in 2012 to prevent leptin inhibition of *in vitro* RM1 prostate cancer cell growth [36]. This observation suggested that insulin could promote cancer cell growth only if its serum concentrations were high enough to overcome the inhibitory effects of leptin on cancer cell growth.

In summary, our observations on the changes in the regulation of the expression of p27 were consistent with the results of the previously published studies where homozygous leptin receptor deficient obese Zucker rats and homozygous long-lived Ames dwarf mice were used [1–7,10,11]. Our observations were also generally consistent with the results of the studies where RM1 murine prostate cancer cells were injected subcutaneously into the obese ob/ob and db/db mice [8]. Our observations were, however, only partially consistent with the results of the studies where MMTV-Wnt-1 mammary tumors were orthotopically transplanted into the right mammary fat pad of obese ob/ob and db/db mice [9]. This problem, however, might be resolved in these animals if the antagonistic relationships between insulin and leptin on cancer cell growth would be taken into consideration.

Acknowledgments

The author is greatly indebted to Dr. Andrzej Bartke at the Southern Illinois University (SIU) School of Medicine (Springfield, IL, USA) for having kindly and generously provided us with homozygous (*Prop1^{-/-}*) long-lived Ames dwarf mice and heterozygous (*Prop1^{+/-}*) Ames normal control mice. The author is also extremely grateful to Mrs. Maryellen Williams and Mrs. Zhaojing Cindy Zeng at the University of Alabama at Birmingham (Birmingham, AL, USA) for performing metabolite analyses of the rodent sera and the University of California Davis Molecular Structure Facility (Davis, CA, USA) for determining the serum levels of free amino acids in mice. Additionally, the author greatly appreciates the research environment provided by the Nutrition Obesity Research Center (P30 DK056336) and the Diabetes Research and Training Center (P60 DK079626), both at the University of Alabama at Birmingham (UAB) (Birmingham, AL, USA). The content of this study, however, is solely the responsibility of the author and does not necessarily represent the official views of the National Institutes of Health or the National Institute of Diabetes and Digestive and Kidney Diseases.

Abbreviations

4E-BP1

eukaryotic translation initiation factor 4E binding protein 1

AICAR	5-amino-4-imidazolecarboxamide riboside
AMPK	5'-AMP-activated protein kinase
CDI	cyclin-dependent kinase inhibitor
CDK	cyclin-dependent kinase
ERK	ERK MAP kinase
GAPDH	glyceraldehydes phosphate dehydrogenase
H & E staining	hematoxylin and eosin staining
MALDI	matrix-assisted laser desorption/ionization
MAPK	mitogen-activated protein kinase
MEK	mitogen-activated protein (MAP) kinase kinase
MNK	MAP kinase interacting kinase
MNU	<i>N</i> -methyl- <i>N</i> -nitrosourea
MS	mass spectrometry
mTOR	mammalian target of rapamycin
nano LC-MS/MS	nano liquid chromatography–tandem mass spectrometry
p21	p21Cip1/Waf1
p27	p27Kip1
PI3K	phosphoinositide 3-kinase
PKB	protein kinase B
RTK	receptor tyrosine kinase
S6K	p70 S6 kinase
TOF	time-of-flight
TSC	tuberous sclerosis complex

REFERENCES

1. Hakkak R, Holley AW, Bunn RC, et al. Effects of obesity on serum insulin growth factor 1 (IGF-1) levels in lean and obese female Zucker rats following DMBA treatment. *FASEB J.* 2005; 19:A993.
2. Hakkak R, Holley AW, Gno F, et al. Effects of obesity on serum adiponectin levels and breast cancer development in lean and obese female Zucker rats following DMBA treatment. *FASEB J.* 2005; 19:A993.
3. Hakkak R, Holley AW, MacLeod S, et al. Obesity promotes DMBA induced mammary tumor development in female Zucker rats. *FASEB J.* 2005; 19:A774.
4. Hakkak R, Holley AW, MacLeod S, et al. Obesity promotes 7,12-dimethylbenz(a)anthracene-induced mammary tumor development in female Zucker rats. *Breast Cancer Res.* 2005; 7:R627–R633. [PubMed: 16168107]
5. Hakkak R, Shaaf S, MacLeod S, et al. Effects of obesity on serum DHEA and DHEA sulfate levels using the obese Zucker rat as a model for breast cancer development. *Obesity.* 2006; 14:A134.
6. Hakkak R, MacLeod S, Shaaf S, et al. Obesity increases the incidence of 7,12-dimethylbenz(a)anthracene-induced mammary tumors in ovariectomized Zucker rat. *Int J Oncol.* 2007; 30:557–563. [PubMed: 17273756]

7. Whitehead T, Holley AW, Kieber-Emmons T, et al. Metabolic phenotype of the DMBA-induced mammary tumor in obese female Zucker rats. *Am Assoc Cancer Res.* 2005; 46:6074.
8. Ribeiro AM, Andrade S, Pinho F, et al. Prostate cancer cell proliferation and angiogenesis in different obese mice models. *Int J Exp Path.* 2010; 91:374–386. [PubMed: 20666851]
9. Zheng Q, Dunlap SM, Zhu J, et al. Leptin deficiency suppresses MMTV-Wnt-1 mammary tumor growth in obese mice and abrogates tumor initiating cell survival. *Endocr Relat Cancer.* 2011; 18:491–503. [PubMed: 21636700]
10. Ikeno Y, Bronson RT, Hubbard GB, et al. Delayed occurrence of fatal neoplastic diseases in Ames dwarf mice: correlation to extended longevity. *J Gerontol Ser A.* 2003; 58:B291–B296.
11. Sharp ZD, Bartke A. Evidence for down-regulation of phosphoinositide 3-kinase/Akt/mammalian target of rapamycin (PI3K/Akt/mTOR)-dependent translation regulatory signaling pathways in Ames dwarf mice. *J Gerontol Ser A.* 2005; 60:293–300.
12. Bielschowsky F, Bielschowsky M. Carcinogenesis in the pituitary of dwarf mouse. The response to dimethylbenzanthracene applied to the skin. *Br J Cancer.* 1961; 15:257–262. [PubMed: 21772452]
13. Alkarain A, Slingerland J. Deregulation of p27 by oncogenic signaling and its prognostic significance in breast cancer. *Breast Cancer Res.* 2004; 6:13–21. [PubMed: 14680481]
14. Eto I. Nutritional and chemopreventive anti-cancer agents up-regulate expression of p27Kip1, a cyclin-dependent kinase inhibitor, in mouse JB6 epidermal and human MCF7, MDA-MB-321 and AU565 breast cancer cells. *Cancer Cell Int.* 2006; 6(20):1–19. [PubMed: 16436212]
15. Eto I. Upstream molecular signaling pathways of p27(Kip1) expression: effects of 4-hydroxytamoxifen, dexamethasone, and retinoic acids. *Cancer Cell Int.* 2010; 10(3):1–19. [PubMed: 20142996]
16. Eto I. Upstream molecular signaling pathways of p27(Kip1) expression in human breast cancer cells *in vitro*: differential effects of 4-hydroxytamoxifen and deficiency of either D-(+)- glucose or L-leucine. *Cancer Cell Int.* 2011; 11(31):1–17. [PubMed: 21214935]
17. Goepfert U, Kullmann M, Hengst L. Cell cycle-dependent translation of p27 involves a responsive element in its 5'-UTR that overlaps with a uORF. *Hum Mol Genet.* 2003; 12:1767–1779. [PubMed: 12837699]
18. Agrawal D, Hauser P, McPherson F, et al. Repression of p27(kip1) synthesis by PDGF in balb/c 3 T3 cells. *Mol Cell Biol.* 1996; 16:4327–4336. [PubMed: 8754833]
19. Hengst L, Reed SI. Translational control of p27Kip1 accumulation during the cell cycle. *Science.* 1996; 71:1861–1864. [PubMed: 8596954]
20. Millard SS, Yan JS, Nguyen H, et al. Enhanced ribosomal association of p27(Kip1) mRNA is a mechanism contributing to accumulation during growth arrest. *J Biol Chem.* 1997; 272:7093–7098. [PubMed: 9054402]
21. Hengst L. A second RING to destroy p27^{Kip1}. *Nature Cell Biol.* 2004; 6:1153–1155. [PubMed: 15573093]
22. Pagano M, Tam SW, Theodoras AM, et al. Role of the ubiquitin-proteasome pathway in regulating abundance of the cyclin-dependent kinase inhibitor p27. *Science.* 1995; 269:682–685. [PubMed: 7624798]
23. Hara T, Kamura T, Nakayama K, et al. Degradation of p27(Kip1) at the G(0)–G(1) transition mediated by a Skp2-independent ubiquitination pathway. *J Biol Chem.* 2001; 276:48937–48943. [PubMed: 11682478]
24. Malek NP, Sundberg H, McGrew S, et al. A mouse knock-in model exposes sequential proteolytic pathways that regulate p27Kip1 in G1 and S phase. *Nature.* 2001; 413:323–327. [PubMed: 11565035]
25. Soos TJ, Kiyokawa H, Yan JS, et al. Formation of p27-CDK complexes during the human mitotic cell cycle. *Cell Growth Differ.* 1996; 7:135–146. [PubMed: 8822197]
26. Rodier G, Montagnoli A, Di Marcotullio L, et al. p27 cytoplasmic localization is regulated by phosphorylation on Ser10 and is not a prerequisite for its proteolysis. *EMBO J.* 2001; 20:6672–6682. [PubMed: 11726503]
27. Viglietto G, Motti ML, Bruni P, et al. Cytoplasmic relocalization and inhibition of the cyclin-dependent kinase inhibitor p27(Kip1) by PKB/Akt-mediated phosphorylation in breast cancer. *Nat Med.* 2002; 8:1136–1144. [PubMed: 12244303]

28. Liang J, Zubovitz J, Petrocelli T, et al. PKB/Akt phosphorylates p27, impairs nuclear import of p27 and opposes p27-mediated G1 arrest. *Nat Med.* 2002; 8:1153–1160. [PubMed: 12244302]
29. Shin I, Yakes FM, Rojo F, et al. PKB/Akt mediates cell-cycle progression by phosphorylation of p27(Kip1) at threonine 157 and modulation of its cellular localization. *Nat Med.* 2002; 8:1145–1152. [PubMed: 12244301]
30. Connor MK, Kotchetkov R, Cariou S, et al. CRM1/RAN-mediated nuclear export of p27^{Kip1} involves a nuclear export signal and links p27 export and proteolysis. *Mol Biol Cell.* 2003; 14:201–213. [PubMed: 12529437]
31. Ciarallo S, Subramanian V, Hung W, Lee JH, Kotchetkov R, Sandhu C, et al. Altered p27Kip1 phosphorylation, localization, and function in human epithelial cells resistant to transforming growth factor β -mediated G1 arrest. *Mol Cell Biol.* 2002; 22:2993–3002. [PubMed: 11940657]
32. Chu I, Sun J, Arnaout A, et al. p27 phosphorylation by Src regulates inhibition of cyclin E-Cdk2. *Cell.* 2007; 128:281–294. [PubMed: 17254967]
33. Kazi A, Carie A, Blaskovich MA, Bucher C, Thai V, Moulder S, et al. Blockade of protein geranylgeranylation inhibits Cdk2-dependent p27Kip1 phosphorylation on Thr187 and accumulates p27Kip1 in the nucleus: implications for breast cancer therapy. *Mol Cell Biol.* 2009; 29:2254–2263. [PubMed: 19204084]
34. Leclerc I, Lenzner C, Gourdon L, Vaulont S, Kahn A, Viollet B. Hepatocyte nuclear factor-4 α involved in type 1 maturity-onset diabetes of the young is a novel target of AMP-activated protein kinase. *Diabetes.* 2001; 50:1515–1521. [PubMed: 11423471]
35. Viollet B, Mounier R, Leclerc J, et al. Targeting AMP-activated protein kinase as a novel therapeutic approach for the treatment of metabolic disorders. *Diabetes Metab.* 2007; 33:395–402. [PubMed: 17997341]
36. Ribeiro AM, Andrade S, Pinho F, et al. Insulin prevents leptin inhibition of RM1 prostate cancer cell growth. *Path Oncol Res.* 2012; 18:499–507. [PubMed: 22113454]
37. Li X, Grundy SM, Patel SB. Obesity in db and ob animals leads to impaired hepatic very low density lipoprotein secretion and differential secretion of apolipoprotein B-48 and B-100. *J Lipid Res.* 1997; 38:1277–1278. [PubMed: 9254055]
38. Wang Z, Al-Regaiey KA, Masternak MM, et al. Adipocytokines and lipid levels in Ames dwarf and calorie-restricted mice. *J Gerontol A Biol Sci Med Sci.* 2006; 61:323–331. [PubMed: 16611697]

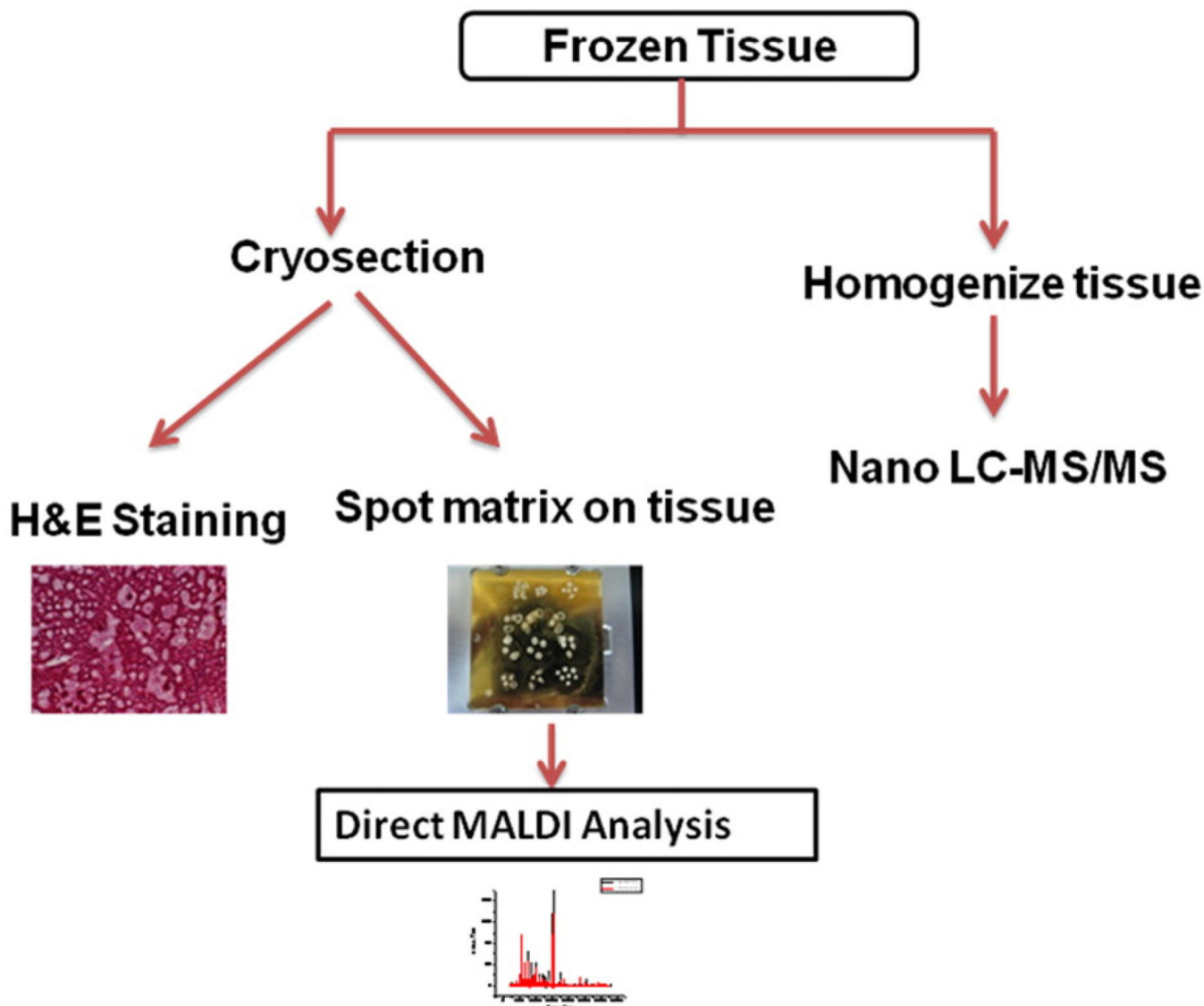


Fig. 1. Workflow for the proteomic analysis of the liver samples. The cryosectioned samples were subjected to (a) hematoxylin and eosin (H & E) staining and (b) differential proteomic profiling analysis by direct matrix-assisted laser desorption/ionization (MALDI) time-of-flight (TOF) mass spectrometry (MS). The homogenized liver samples were subjected to the differential proteomic identification analysis by nano liquid chromatography–tandem mass spectrometry (nano LC-MS/MS). Nano LC-MS/MS method was used because it tended to produce far fewer false positives than the conventional two dimensional (2D)-Gel method.

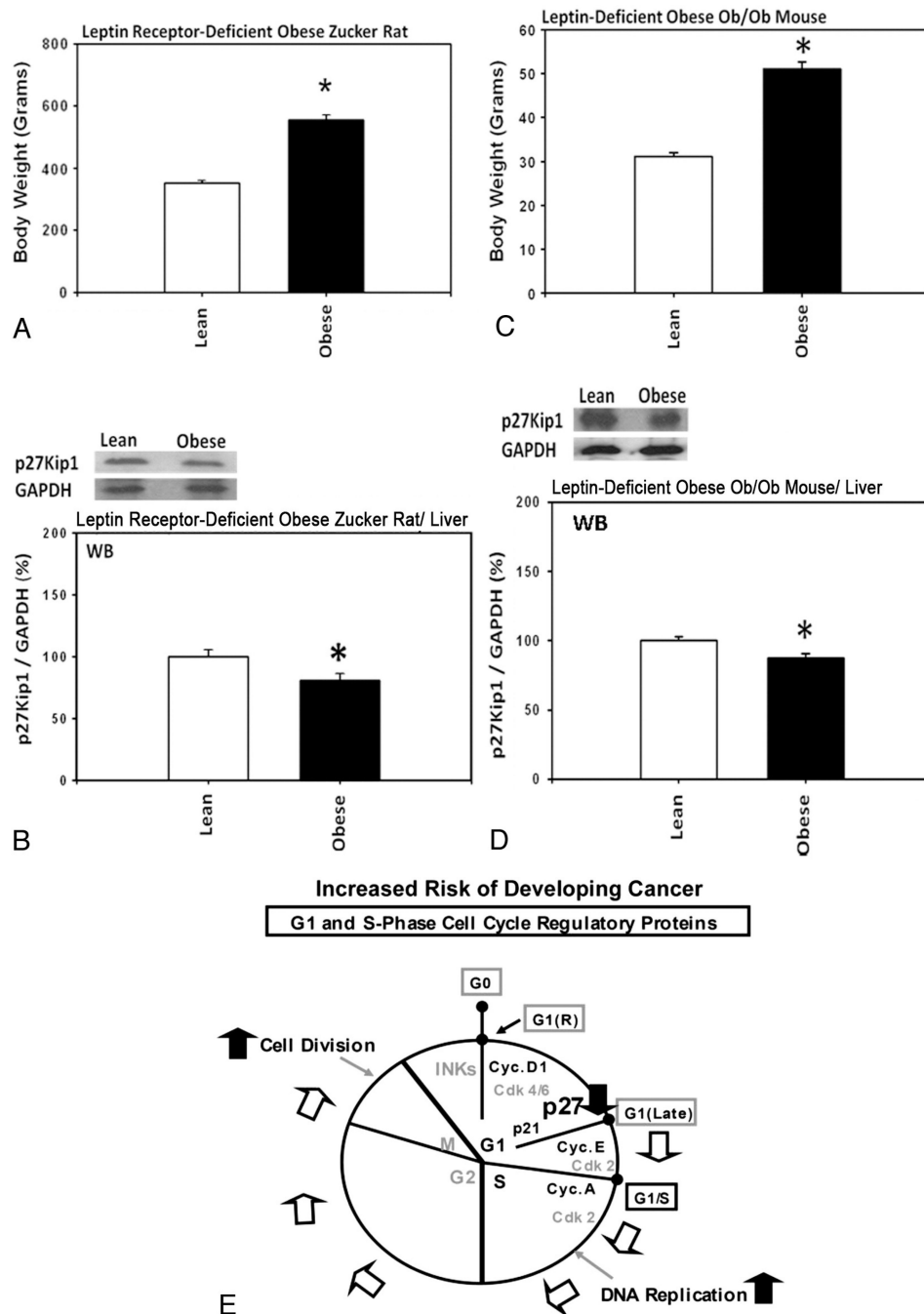


Fig. 2. Homozygous leptin receptor-deficient obese Zucker rats and homozygous leptin-deficient obese ob/ob mice had significantly higher body weights and the levels of the hepatic expression of p27 were significantly lower compared with heterozygous lean controls. (A) Body weights of the obese Zucker rats (n=3) and the lean control Zucker rats (n=3). (B) Levels of the hepatic expression of p27 in the obese Zucker rats (n=3) and the lean control Zucker rats (n=3). (C) Body weights of the obese ob/ob mice (n=3) and the lean control mice (n=3). (D) Levels of the hepatic expression of p27 in the obese ob/ob mice (n=3) and the lean control mice (n=3). (E) A hypothetical diagram showing how the lower levels of the expression of p27 could increase the risk of developing cancer.

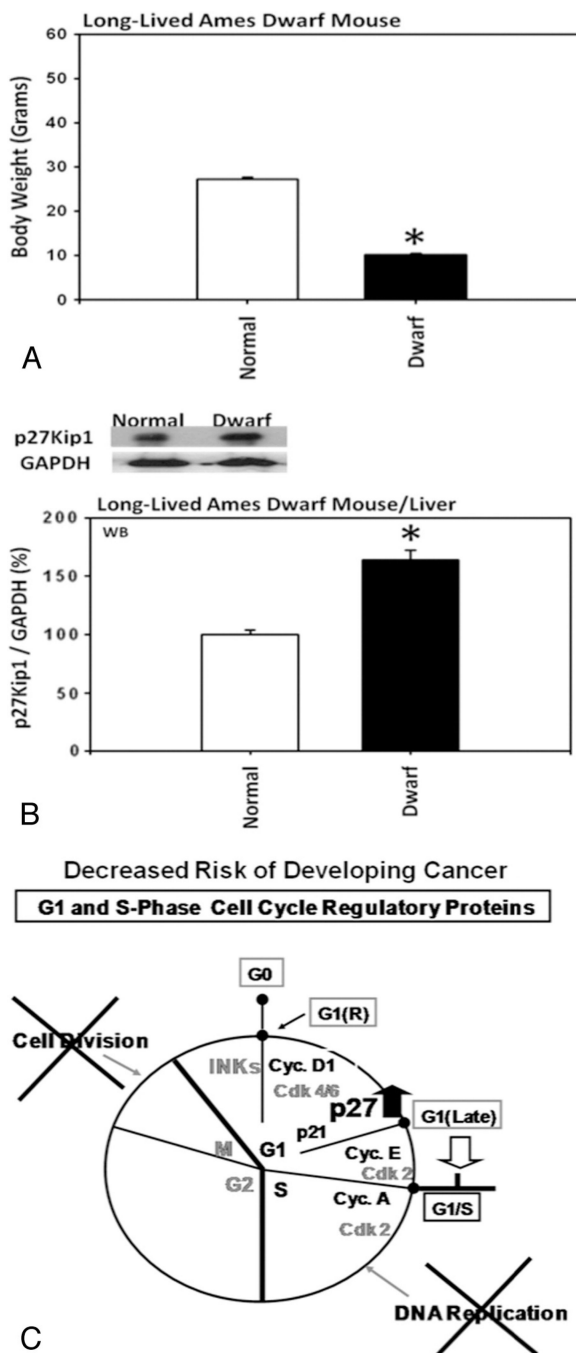


Fig. 3. Homozygous long-lived Ames dwarf mice had significantly lower body weights and significantly higher levels of the hepatic expression of p27 compared with heterozygous Ames normal control mice. (A) Body weights of the long-lived Ames dwarf mice (n=3), and Ames normal control mice (n=3). (B) Levels of the hepatic expression of p27 in the long-lived Ames dwarf mice (n=3), and Ames normal control mice (n=3). (C) A hypothetical diagram showing how the higher levels of the expression of p27 could decrease, rather than increase, the risk of developing cancer.

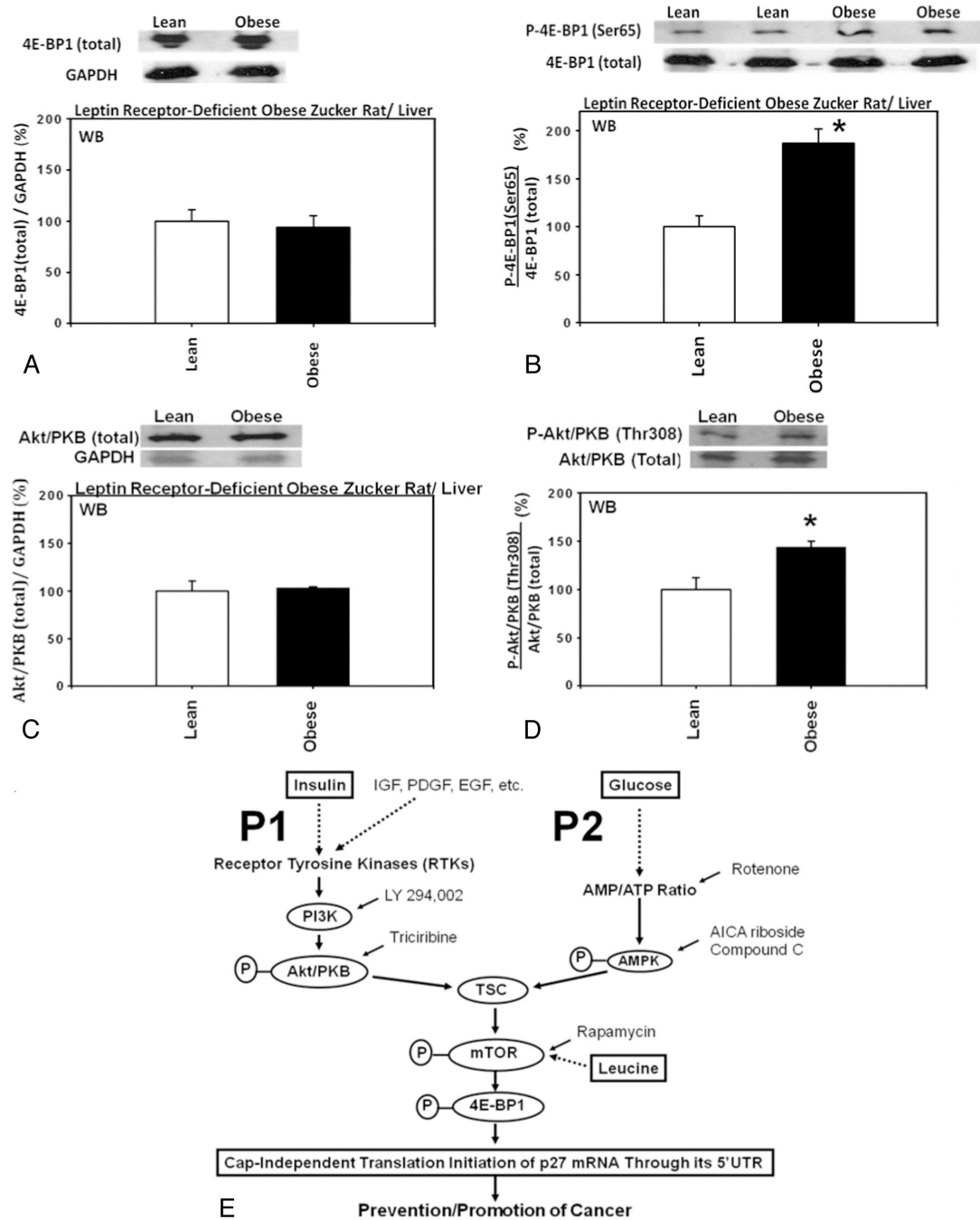


Fig. 4.

Upstream molecular signaling pathways for the expression of p27 were down-regulated in the livers from homozygous leptin receptor-deficient obese Zucker rats compared with heterozygous lean control Zucker rats. Hepatic expression of (A) total 4E-BP1 (n=3 each for experimentals and controls), (B) 4E-BP1 phosphorylated at Ser65 (n=3 each for experimentals and controls), (C) total Akt/PKB (n=3 each for experimentals and controls) and (D) Akt/PKB phosphorylated at Thr308 (n=3 each for experimentals and controls) in the homozygous leptin receptor-deficient obese Zucker rats compared with heterozygous lean control Zucker rats. (E) Outline of the upstream molecular signaling pathways for the expression of p27.

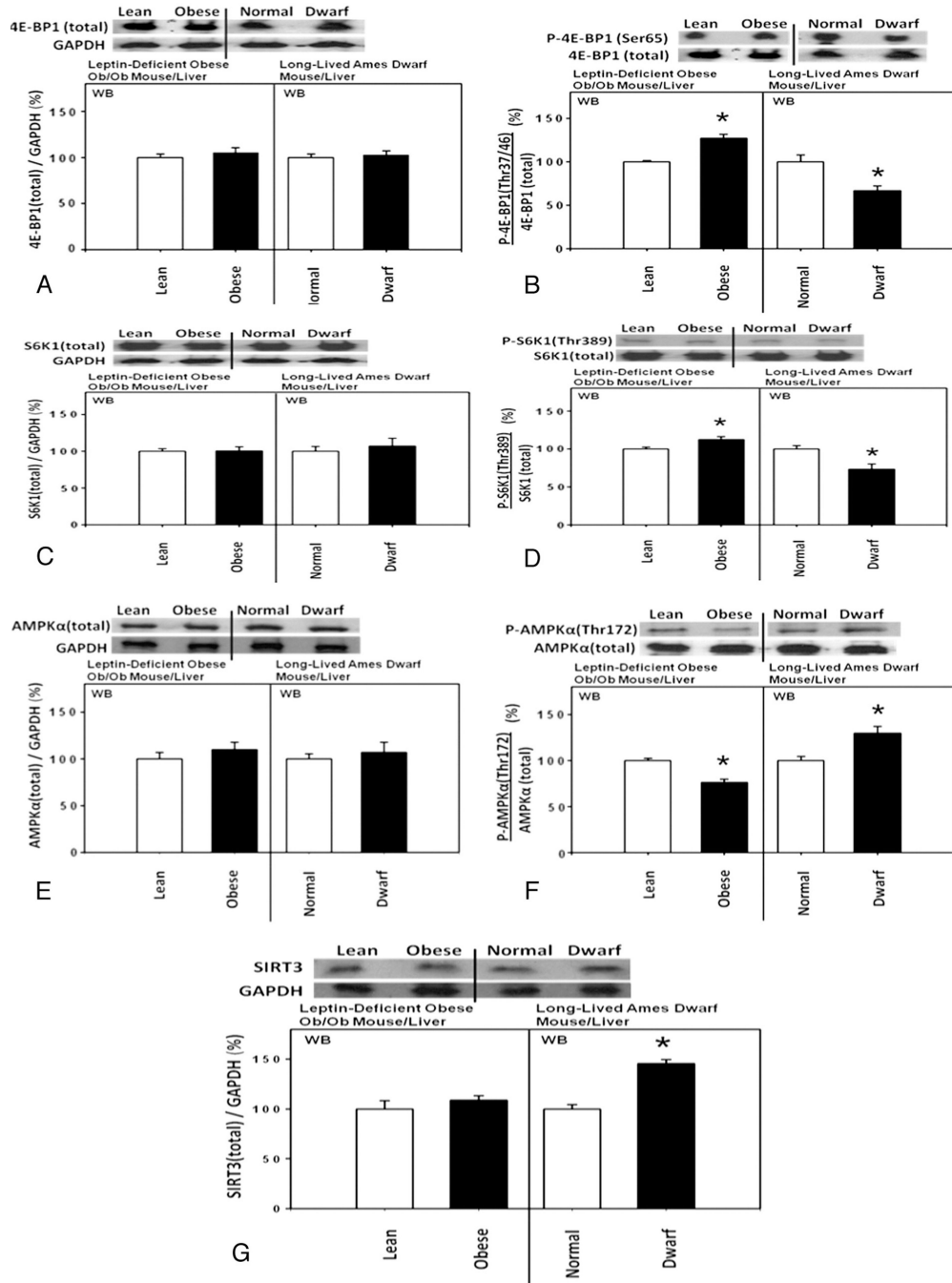


Fig. 5. Upstream molecular signaling pathways for the expression of p27 were down-regulated in the livers from homozygous leptin-deficient obese ob/ob mice compared with heterozygous lean control mice. By contrast, the direction of the changes in the hepatic expression of these proteins was opposite in homozygous long-lived Ames dwarf mice compared with heterozygous Ames normal control mice. Hepatic expression of (A) total 4E-BP1 (n=3 each for experimentals and controls), (B) 4E-BP1 phosphorylated at Thr37/46 (n=3 each for experimentals and controls), (C) total S6K1 (n=3 each for experimentals and controls) and (D) S6K1 phosphorylated at Thr389 (n=3 each for experimentals and controls), (E) total AMPKα (n=3 each for experimentals and controls), (F) AMPKα phosphorylated at Thr172

(n=3 each for experimentals and controls), and (G) SIRT3 (n=3 each for experimentals and controls) in the homozygous leptin-deficient obese ob/ob mice, heterozygous lean control mice, homozygous long-lived Ames dwarf mice and heterozygous Ames normal control mice.

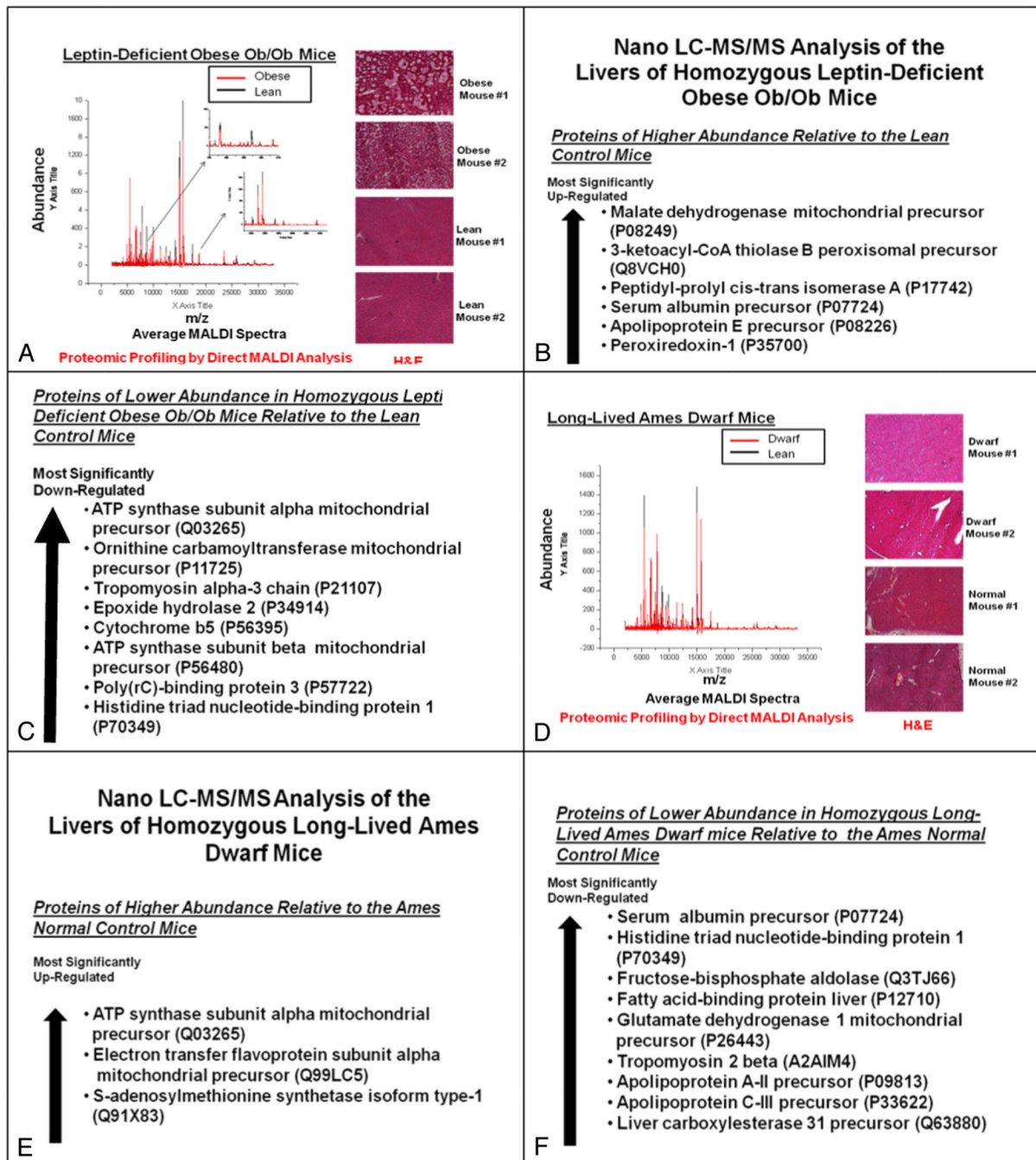


Fig. 6. Proteomic analysis of the upstream molecular signaling pathways for the hepatic expression of p27 in the homozygous leptin-deficient ob/ob mice and homozygous long-lived Ames dwarf mice compared with heterozygous lean and normal control mice, respectively. (A and D) Differential proteomic profiling analysis – by direct matrix-assisted laser desorption/ionization (MALDI) time-of-flight (TOF) mass spectrometry (MS) – and hematoxylin and eosin (H & E) staining of the cryosectioned liver samples from (A) homozygous leptin-deficient ob/ob mice (n=5 each for experimentals and controls) and (D) homozygous long-lived Ames dwarf mice (n=5 each for experimentals and controls). (B, C, E, and F) Differential proteomic identification analysis – by nano liquid chromatography–tandem

mass spectrometry (nano LC-MS/MS) – of the homogenized liver samples from (B and C) homozygous leptin-deficient ob/ob mice (n=5 each for experimentals and controls) and (E and F) homozygous long-lived Ames dwarf mice (n=5 each for experimentals and controls).

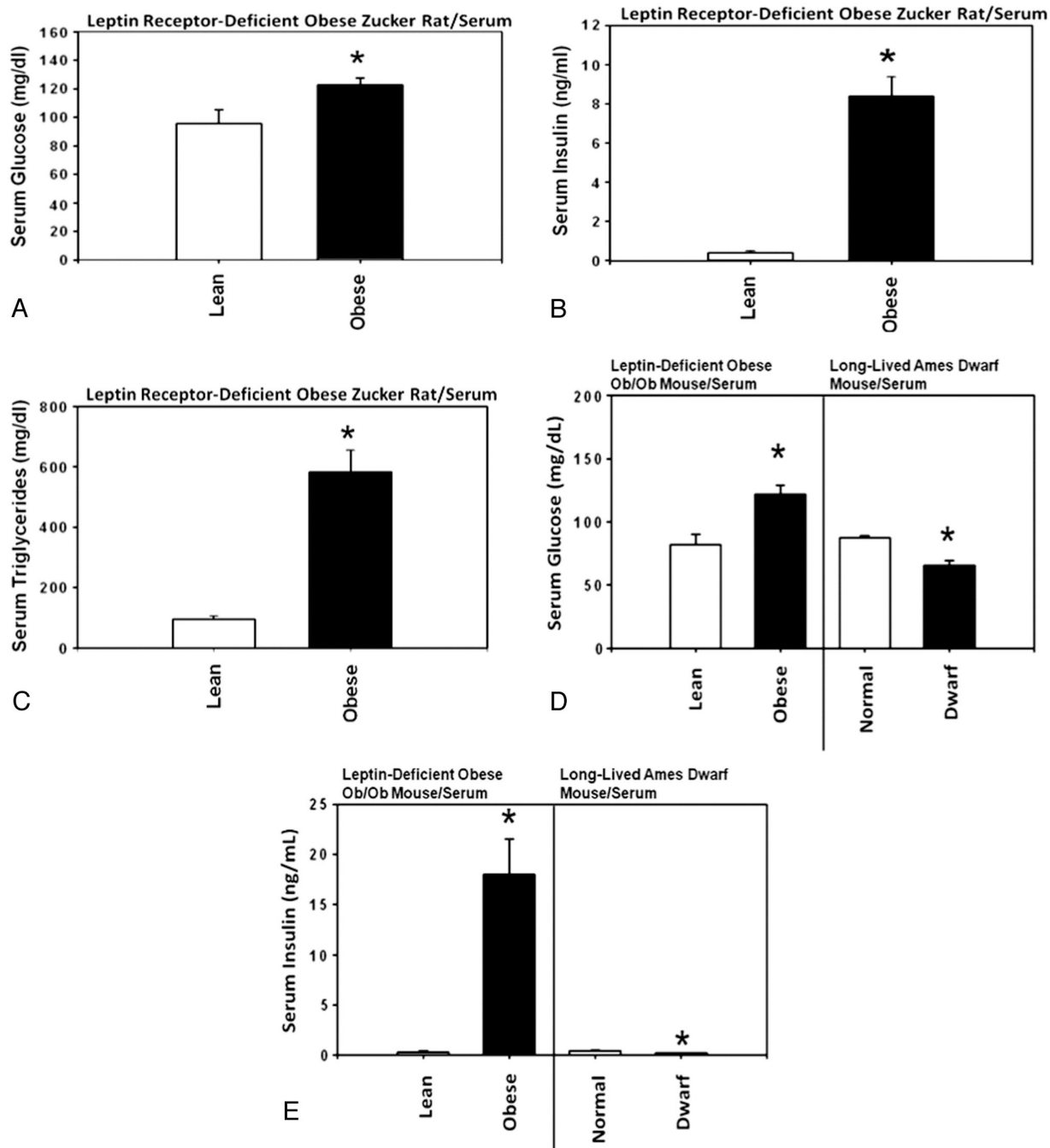


Fig. 7. Analysis of the serum levels of glucose, insulin, triglycerides and free amino acids in homozygous leptin receptor-deficient obese Zucker rats, leptin-deficient obese ob/ob mice and long-lived Ames dwarf mice. Serum concentrations of (A) glucose, (B) insulin and (C) triglycerides in homozygous leptin receptor-deficient obese Zucker rats (n=5) compared with heterozygous lean control Zucker rats (n=5), and (D) glucose and (E) insulin in homozygous leptin-deficient obese ob/ob mice (n=5) and homozygous long-lived Ames dwarf mice (n=5) compared with heterozygous lean and normal control mice (n=5 each), respectively.

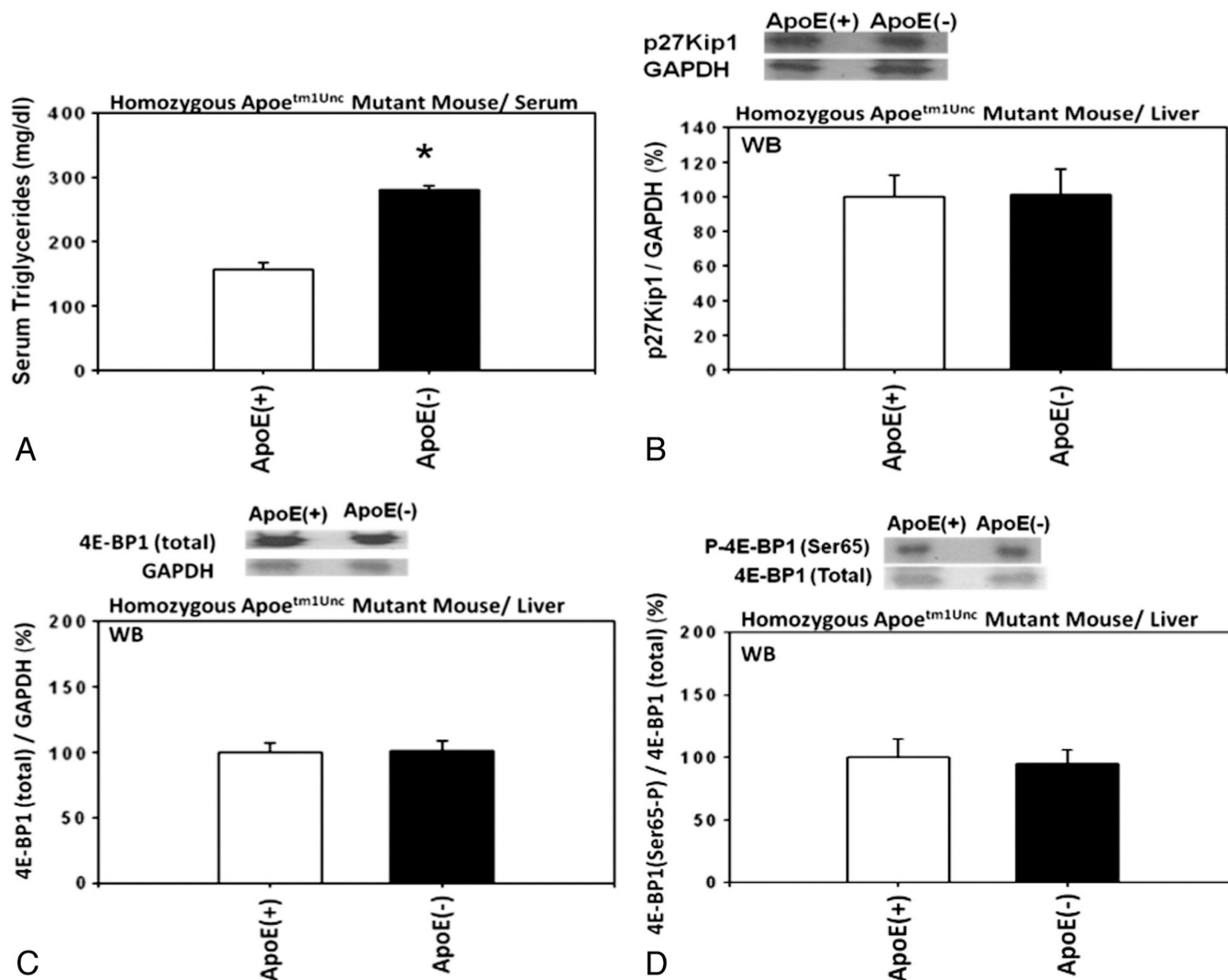


Fig. 8. Serum levels of triglycerides and hepatic expression of p27 and 4E-BP1 phosphorylated at Ser65 in *ApoE^{tm1Unc}* mutant mice. (A) Serum levels of triglycerides in homozygous *ApoE^{tm1Unc}* mutant mice on C57BL/6 background (n=5) compared with wild-type C57BL/6 mice (n=5). Hepatic expression of (B) p27, (C) total 4E-BP1, and (D) 4E-BP1 phosphorylated at Ser65 in the homozygous *ApoE^{tm1Unc}* mutant mice on C57BL/6 background (n=3) compared with wild-type C57BL/6 mice (n=3).

Serum levels of free amino acids in leptin-deficient obese ob/ob mice and long-lived Ames dwarf mice. The levels of free amino acids were determined in the serum of homozygous leptin-deficient obese ob/ob mice (n=5), heterozygous lean control mice (n=5), homozygous long-lived Ames dwarf mice (n=5) and heterozygous Ames normal control mice (n=5).

Table 1

	Leptin-Deficient Obese Ob/Ob Mice				Long-Lived Ames Dwarf Mice				
	Lean Control (n=5)		Obese (n=5)		Normal Control (n=5)		Dwarf (n=5)		
	Mean (μmol/100 ml)	S.E.M.	Mean (μmol/100 ml)	S.E.M.	Mean (μmol/100 ml)	S.E.M.	Mean (μmol/100 ml)	S.E.M.	
TOTAL AMINO ACIDS	251.61	4.70	370.31	22.01	335.24	12.05	309.96	###	NS
INDIVIDUAL AMINO ACIDS									
Totally indispensable									
Threonine	9.96	0.26	13.67	0.74	13.73	1.16	14.20	1.45	NS
Lysine	22.52	0.75	26.10	1.91	20.70	1.85	13.23	1.13	*
Carbon-skeleton indispensable									
Phenylalanine	10.53	0.29	19.36	0.78	18.66	0.39	24.62	4.33	NS
Branched-chain amino acids									
Valine	19.46	0.81	27.43	0.79	25.00	0.91	19.32	1.56	*
Isoleucine	16.57	0.79	21.91	0.65	21.52	0.68	17.35	1.87	*
Leucine	9.87	0.45	13.65	0.53	11.77	0.66	8.56	0.76	NS
Methionine	3.49	0.05	3.81	0.39	12.34	1.01	44.18	8.15	*
Histidine	6.37	0.09	7.51	0.57	6.00	1.10	5.08	0.32	NS
Tryptophan	4.64	1.79	7.34	0.73	11.03	1.61	9.83	1.60	NS
Conditionally or acquired indispensable									
Tyrosine	5.16	0.29	7.43	0.54	6.61	0.32	6.14	0.51	NS
Cysteine	0.07	0.07	0.29	0.29	0.17	0.17	0.15	0.15	NS
Arginine	11.12	0.65	3.45	2.30	15.49	1.89	5.87	0.87	*** ↓↓
Glutamine	6.27	0.28	15.87	4.49	8.21	0.99	9.09	0.30	NS
Dispensable									
Alanine	22.86	0.94	58.69	5.13	46.32	0.61	38.92	2.57	*
Serine	8.07	0.43	12.63	0.56	10.32	1.25	11.45	1.81	NS

	Leptin-Deficient Obese Ob/Ob Mice				Long-Lived Ames Dwarf Mice						
	Lean Control (n = 5)		Obese (n = 5)		Normal Control (n = 5)		Dwarf (n = 5)		P		
	Mean	S.E.M.	Mean	S.E.M.	Mean	S.E.M.	Mean	S.E.M.			
	($\mu\text{mol}/100\text{ ml}$)	($\mu\text{mol}/100\text{ ml}$)	($\mu\text{mol}/100\text{ ml}$)	($\mu\text{mol}/100\text{ ml}$)	($\mu\text{mol}/100\text{ ml}$)	($\mu\text{mol}/100\text{ ml}$)	($\mu\text{mol}/100\text{ ml}$)	($\mu\text{mol}/100\text{ ml}$)			
Asparagine	1.25	0.12	1.99	0.07	**	††	1.80	0.10	0.87	0.39	NS
Proline	6.25	0.11	8.39	0.43	**	††	10.06	0.78	9.17	0.87	NS
Aspartic acid	1.47	0.25	1.89	0.37	NS		1.75	0.30	1.39	0.73	NS
Glutamic acid	65.80	2.29	98.52	14.82	NS		73.97	3.77	42.71	5.12	** ↓↓
Glycine	19.89	0.71	20.40	2.71	NS		19.81	1.85	27.82	1.63	* ↑
NON-AMINO ACIDS											
Urea cycle											
Omithine	5.92	0.24	21.78	1.14	****	††††	8.08	0.56	11.52	1.31	NS
Citrulline	4.32	0.21	8.41	2.21	NS		6.71	0.43	5.93	0.48	NS
Ammonia	25.04	2.81	34.25	3.35	NS		12.44	0.87	18.46	3.16	NS
Methionine-transsulfuration pathways											
Cystathionine	0.69	0.06	0.70	0.06	NS		1.81	0.23	0.47	0.39	* ↓
Taurine	83.75	3.59	199.44	60.62	NS		75.66	11.50	83.21	6.43	NS
Ethanolamine	3.54	0.56	4.24	0.45	NS		1.21	1.21	3.55	1.79	NS
Phosphoethanolamine	0.00	0.00	0.00	0.00	-		0.00	0.00	0.00	0.00	-
Homocystine (half)	0.00	0.00	0.00	0.00	-		0.00	0.00	0.00	0.00	-
Other											
Hydroxyproline	1.95	0.13	1.39	0.05	*	↓	1.75	0.44	1.21	0.62	NS
3-Methylhistidine	1.52	0.15	1.93	0.20	NS		3.59	1.02	1.88	0.31	NS
Sarcosine	0.00	0.00	78.45	78.45	NS		0.00	0.00	0.00	0.00	-
Carnosine	0.00	0.00	0.00	0.00	-		5.97	3.23	0.00	0.00	NS

NS: Not significant;

* P < 0.05 ↑ or ↓;

** P < 0.01 ↑↑ or ↓↓;

*** P < 0.005 ↑↑↑ or ↓↓↓;

P < 0.001 ↑↑↑ or ↓↓↓.

↑ Higher levels in the serum of experimental mouse relative to the control mouse.

↓ Lower levels in the serum of experimental mouse relative to the control mouse.

Eto